

A DFT Study on Reaction of Eupatilin with Hydroxyl Radical in Solution

Minjie Li,^{*,[a]} Weixia Liu,^[a] Chunrong Peng,^[a] Qinghua Ren,^[a] Wencong Lu,^[a] and Wei Deng^[b]

Antioxidants scavenge reactive oxygen species and, therefore, are vitally important in the living cells. The antioxidant properties of eupatilin have recently been reported. In this article, the reactions of eupatilin with the hydroxyl radical (OH[•]) in solution are studied using density functional theory calculations and the polarizable continuum model. Three mechanisms are considered including: sequential electron proton transfer (SEPT), sequential proton loss electron transfer (SPLET), and hydrogen abstraction (HA). Three solvents with different polarities, that is, benzene, methanol, and water, are used to investigate the effect of the environment on the mechanisms. The relative Gibbs free energies and enthalpies corresponding to different mechanisms are calculated. Our results show that SEPT is thermodynamically favored in aqueous

solution. Once the eupatilin anion is produced, the second step in SPLET mechanism is thermodynamically favored in methanol and water. The HA mechanism is thermodynamically favored in gas, benzene, methanol, and water. This mechanism is more energetically favorable to occur in a more polar solvent. The natural bond orbital charges and spin densities as well as the singly occupied molecular orbital are then analyzed. It is concluded that the HA process is governed by proton coupled electron transfer mechanism. The attack of the radical takes place preferentially at position 7 of eupatilin. © 2012 Wiley Periodicals, Inc.

DOI: 10.1002/qua.24060

Introduction

Reactive oxygen species (ROS), such as hydroxyl radical (OH[•]), peroxy radical (RO₂[•]), alkoxyl radical (RO[•]) (R = alkyl group), and superoxide radical anion (O₂^{•-}), are constantly formed in living organisms due to γ , X-rays, and UV radiations.^[1–3] These species are highly reactive. Among all the ROS, the hydroxyl radical OH[•] is the most common and most reactive. It can seriously alter our biological constituents like lipid, cell membrane, DNA, and protein when the radical is generated in excess or not appropriately controlled by antioxidants. The chemical damage is commonly referred to as oxidative stress and is responsible for various diseases such as cancer, atherosclerosis, and Alzheimer's disease.^[4–10]

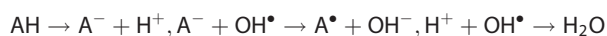
Eupatilin (5,7-dihydroxy-3',4',6-trimethoxyflavone, Eupa, Fig. 1) is a pharmacologically active flavonoid isolated from medicinal herbs of *Artemisia asiatica*. It has been shown to exert antitumor, anti-inflammatory, and antioxidative activities.^[11–23] It may be used as a potential cancer chemopreventive agent and as an antioxidant inhibiting the ROS damage.^[13–15,19–21] For example, eupatilin can induce G2/M cell cycle to arrest in human endometrial cancer cells, increase the activation of ERK1/2, and decrease the activation of Akt in Hec1A cells. Thus, it could be considered a potential therapeutic and chemopreventive agent for the treatment of human endometrial cancer.^[20] It has also been shown to be a competitive inhibitor of CYP1A2 in human liver microsomes.^[17] It inhibits H₂O₂-induced apoptotic cell death through inhibition of mitogen-activated protein kinases and nuclear factor- κ B(7).^[14] Similarly, eupatilin can inhibit ROS production and protect gastric epithelial cells from oxidative damage.^[13]

Recently, eupatilin has been reported to be effective in scavenging of ROS in human breast epithelial cells.^[19] It is important to study the radical scavenging mechanisms of eupatilin with ROS. However, to the best of our knowledge, there is no theoretical study reported so far regarding the scavenging activity of eupatilin toward ROS.

Three mechanisms are commonly proposed to explain radical scavenging processes of phenolic antioxidants, (AH).^[24–35] The first is sequential electron proton transfer (SEPT):



The second is sequential proton loss electron transfer (SPLET):



Finally, the third is hydrogen abstraction (HA), including hydrogen atom transfer (HAT) and proton coupled electron

[a] M. Li, W. Liu, C. Peng, Q. Ren, W. Lu
Department of Chemistry, College of Science, Shanghai University, Shanghai 200444, People's Republic of China
E-mail: minjieli@shu.edu.cn

[b] W. Deng
Research Center of Nano Science and Technology, Shanghai University, Shanghai 200444, People's Republic of China

Contract grant sponsor: National Science Foundation of China; contract grant numbers: 20902056, 21174081, 20973108.

Contract grant sponsor: Leading Academic Discipline Project of Shanghai Municipal Education Commission, China; contract grant number: J50101.

Contract grant sponsor: Innovation Foundation of Shanghai University, China.

© 2012 Wiley Periodicals, Inc.

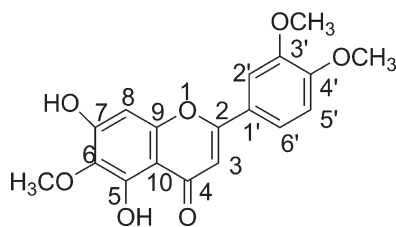
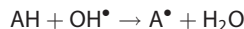


Figure 1. Structure of eupatilin (5,7-dihydroxy-3',4',6'-trimethoxyflavone), including atom numbering.

transfer (PCET) mechanisms:



All the three mechanisms afford the same product, that is, the A^\bullet radical. They may occur in parallel with different rates in a certain biological system.^[26–35] The relative importance of these mechanisms will depend both on the specific chemical properties of the reactants and on the polarity of the solvent in which the reaction takes place.

The aim of this work is to systematically study the mechanisms of the reaction of eupatilin with hydroxyl radical, the most reactive radical in ROS. The structures and energetics of the different species involved in the reaction are determined using the B3LYP/6-311++g(2df,2p)//B3LYP/6-31g(d) method. The solvation effects are treated using the polarizable continuum model (PCM). Three reaction mechanisms, that is, SEPT, HA (included HAT and PCET), and SPLET, are considered, and all possible reaction pathways are investigated in detail. In addition, the influence of the polarity of the solvent on the reactivity is also studied.

Computational Methods

All calculations were performed using Gaussian 03 programs.^[36] Geometry optimizations and frequency calculations were carried out using the B3LYP hybrid density functional^[37] with the 6-31g(d) basis set.^[38] UB3LYP was used for open shell systems. The B3LYP functional has been used successfully for radical scavenging mechanisms.^[32,33,39–44] Local minima and transition states were identified by imaginary frequencies. Thermodynamic corrections were obtained from the frequency calculations. Intrinsic reaction coordinate calculations were performed to confirm that transition states properly connect reactants and products. Single-point electronic energies were then calculated at the B3LYP/6-311++g(2df,2p) level.

Solvent effects were taken into consideration using the self-consistent reaction field method with the polarizable continuum model (PCM)^[45] at B3LYP/6-311++G(d,p) level of theory and RADII = UAHF.^[46,47] Benzene, methanol, and water were chosen as solvents to mimic low, medium, and higher polar environments, with dielectric constants of 2.247, 32.63, and 78.39, respectively. In all cases, the reference state is 1 M, 298 K.^[47] We should note that the method used in this work closely follows that used by Zúñiga's group to study the reaction of β -carotene with the nitrogen dioxide radical in solution^[44] and that used by other groups to study the antioxidant

properties.^[32,33,39–43] To describe the nature of the charge transfer, the natural bond orbital (NBO)^[48] analysis of charges as well as spin densities of the reactants, transition states, and products of the HA mechanism were performed. The distributions of the single occupied molecular orbital (SOMO) were also used to identify the scavenging mechanism.

The relative enthalpy changes corresponding to different mechanism were calculated using following equations:

$$\text{BDE} = H(\text{Eupa}(-\text{H})^\bullet) + H(\text{H}^\bullet) - H(\text{Eupa})$$

$$\text{IP} = H(\text{Eupa}^{\bullet+}) + H(\text{e}^-) - H(\text{Eupa})$$

$$\text{ETE} = H(\text{Eupa}(-\text{H})^\bullet) + H(\text{e}^-) - H(\text{Eupa}(-\text{H})^-)$$

$$\text{PDE} = H(\text{Eupa}(-\text{H})^\bullet) + H(\text{H}^+) - H(\text{Eupa}^{\bullet+})$$

$$\text{PA} = H(\text{Eupa}(-\text{H})^-) + H(\text{H}^+) - H(\text{Eupa})$$

$$\text{EA} = H(\text{OH}^-) - H(\text{e}^-) - H(-\text{OH}^\bullet)$$

where $H = E_0 + \text{ZPE} + \Delta H_{\text{trans}} + \Delta H_{\text{rot}} + \Delta H_{\text{vib}} + RT$.^[49,50] E_0 represents the calculated total electronic energy. ZPE means zero-point energies. ΔH_{trans} , ΔH_{rot} , and ΔH_{vib} are the translational, rotational, and vibrational contributions. The reaction enthalpy changes ($\Delta_r H$) can be obtained as the difference in enthalpies between the products and the reactants.

The total Gibbs free energy was determined using the equation, $G = E_0 + \text{ZPE} + \Delta H_{\text{trans}} + \Delta H_{\text{rot}} + \Delta H_{\text{vib}} + RT - \text{transition state (TS)}$.^[51] The last term, TS , stands for the entropy contribution to the Gibbs free energy. The half reaction Gibbs free energies are computed using following equations:

$$\text{IPG} = G(\text{Eupa}^{\bullet+}) + G(\text{e}^-) - G(\text{Eupa})$$

$$\text{ETG} = G(\text{Eupa}(-\text{H})^\bullet) + G(\text{e}^-) - H(\text{Eupa}(-\text{H})^-)$$

$$\text{PDG} = G(\text{Eupa}(-\text{H})^\bullet) + G(\text{H}^+) - G(\text{Eupa}^{\bullet+})$$

$$\text{PDG} = G(\text{Eupa}(-\text{H})^-) + G(\text{H}^+) - G(\text{Eupa})$$

$$\text{EAG} = G(\text{OH}^-) - G(\text{e}^-) - G(-\text{OH}^\bullet).$$

The reaction Gibbs free energies ($\Delta_r G$) were predicted as the differences between the Gibbs free energies of products and those of reactants.

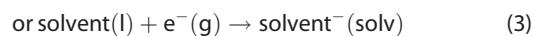
To calculate the half reaction enthalpies and Gibbs free energies, the enthalpies and Gibbs free energies of H-atom (H^\bullet), proton (H^+), and electron (e^-) in gas phase are needed. The gas-phase enthalpy of hydrogen atom predicted using G3B3 method is -312.956 kcal/mol.^[50] The gas-phase enthalpy of proton and electron are 1.483 and 0.752 kcal/mol, respectively.^[52] The gas-phase Gibbs free energies for hydrogen atom (H^\bullet), proton (H^+), and electron (e^-) are -321.123 (predicted by G3B3 method^[50]), -6.3 , and 0 kcal/mol, respectively.^[53,54] The hydration enthalpies and Gibbs free energies are also needed in the calculation of the half reaction enthalpies and Gibbs free energies in solutions. The hydration enthalpies in three solvents and the hydration Gibbs free energies in water are listed in Table 1. Because H^\bullet , H^+ , and e^- solvation Gibbs free energies in methanol and benzene are not available in previous literatures, they are determined as the Gibbs free energy changes in the following processes (1–3)

Table 1. Solvation enthalpies and Gibbs free energies of H[•], H⁺, and e[−] in benzene, methanol, and water solutions (in kcal/mol).

Solvent	$\delta_{\text{solv}}(\text{H}^{\bullet})$	$\delta_{\text{solv}}H(\text{H}^{+})^{\text{[a]}}$	$\delta_{\text{solv}}H(\text{e}^{-})^{\text{[a]}}$	$\delta_{\text{solv}}G(\text{H}^{\bullet})$	$\delta_{\text{solv}}G(\text{H}^{+})$	$\delta_{\text{solv}}G(\text{e}^{-})$
Benzene	1.5 ^[b]	−213.7	−1.7	3.7	−209.0	−0.4
Methanol	1.2 ^[b]	−248.1	−20.6	2.1	−247.3	−17.1
Water	1.0 ^[c]	−244.3	−25.1	3.3 ^[d]	−262.4	−35.5 ^[e]

[a] From the Ref. [55]. [b] From the Ref. [55]. [c] From the Ref. [52,56]. [d] From the Ref. [57]. [e] From the Ref. [54].

reported by Rimarcik group.^[55] The predicted values are given in Table 1.



Here, H[•], H⁺, and e[−] is “attached” to one molecule of solvent which are optimized using IEF-PCM DFT/B3LYP/6-311++G(d,p) method in the same solvent.^[55] Although the potential inaccuracy related to the half reaction enthalpies and Gibbs free energies is introduced by the application of experimental or estimated solvation enthalpies and solvation Gibbs free energies of H[•], H⁺, and e[−], it will be cancel when the reaction enthalpies and reaction Gibbs free energies are predicted. Conversely, the relative values are useful to determine the preferred reaction pathway in the studied solvents.

Results and Discussion

As previously mentioned, phenolic antioxidants can scavenge hydrogen radical commonly through three mechanisms, that is, SEPT, HA, and SPLET. The three mechanisms for the reaction of eupatilin with hydroxyl radical (Fig. 2) in gas phase, benzene, methanol, and water have been studied and the results are pre-

sented and discussed below. All the possible reactive sites of eupatilin including the hydrogen abstracted sites are investigated.

Sequential electron proton transfer

In the SEPT mechanism, the first step is single electron transfer from the antioxidant to hydroxyl radical ($\text{Eupa} + \text{OH}^{\bullet} \rightarrow \text{Eupa}^{+\bullet} + \text{OH}^{-}$), and the second step is the proton dissociation process ($\text{Eupa}^{+\bullet} \rightarrow \text{Eupa}(-\text{H})^{\bullet} + \text{H}^{+}$). To study the viability of the mechanism, we calculate the corresponding changes of the enthalpies and Gibbs free energy for two steps at 298.15 K in gas phase, benzene, methanol, and water solutions. The Gibbs free energy and enthalpy changes of the reaction are reported in Table 2. The corresponding changes of half reaction, the individual contributions of the reactants are given in Table 3.

Gibbs Free Energy Changes As observed, the reaction through the single electron transfer process ($\text{Eupa} + \text{OH}^{\bullet} \rightarrow \text{Eupa}^{+\bullet} + \text{OH}^{-}$, $\Delta_r G$) is thermodynamically favored in the two polar solvents, that is, methanol and water, with negative values of $\Delta_r G = -0.6$ and -3.3 kcal/mol, respectively. The mechanism is forbidden in gas phase and in the nonpolar solvent of benzene with $\Delta_r G = 125.4$ and 63.0 kcal/mol, respectively. In the studied environments, the reaction Gibbs free energies increase in this order: water < methanol < benzene < gas. The more polar the solutions, the more favorable thermodynamically the single electron transfer process. This observation agrees with the results by other studies.^[44,58] In the half reaction of the first

step, the electron transfer from the neutral form of eupatilin ($\text{Eupa} \rightarrow \text{Eupa}^{+\bullet} + \text{e}^{-}$, ionization potentials Gibbs free energy (IPG)) is found to be endergonic, regardless of the polarity of the environment. IPG in gas phase is about 70 kcal/mol higher than that in water. The data increase in the order of: water < methanol < benzene < gas. Although the electron transfer process from neutral form to radical cation form is thermodynamically forbidden, the electron transfer from the hydroxyl radical ($\text{OH}^{\bullet} + \text{e}^{-} \rightarrow \text{OH}^{-}$, electron affinity Gibbs free energy (EAG)) is exergonic independent of the polarity of solvents. The more stable the anionic form (OH^{-}) achieved by the hydroxyl radical (OH^{\bullet}), the more stable the radical

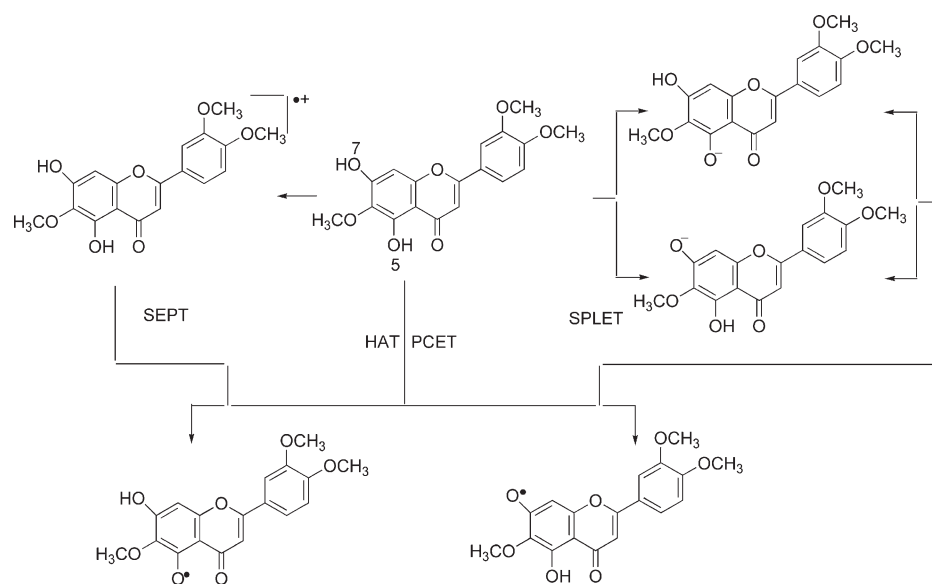
**Figure 2.** All reaction pathways for the reaction of eupatilin with hydroxyl radical.

Table 2. Reaction enthalpy and Gibbs free energy (in kcal/mol) at 298.15 K for SEPT mechanism in gas phase, benzene, methanol and water solutions ($\text{Eupa} + \text{OH}^\bullet \rightarrow \text{Eupa}^{+\bullet} + \text{OH}^-$, and $\text{Eupa}^{+\bullet} \rightarrow \text{Eupa}(-\text{H})^\bullet + \text{H}^+$).

	Gas	Benzene	Methanol	Water
$\Delta_r G_{(\text{Eupa} + \text{OH}^\bullet \rightarrow \text{Eupa}^{+\bullet} + \text{OH}^-)}$	125.4	63.0	-0.6	-3.3
$\Delta_r H_{(\text{Eupa} + \text{OH}^\bullet \rightarrow \text{Eupa}^{+\bullet} + \text{OH}^-)}$	125.8	63.4	-0.2	-2.9
$\text{PDG}_{(\text{Eupa}^{+\bullet} \rightarrow \text{Eupa}(-5\text{H})^\bullet + \text{H}^+)}$	232.7	37.6	10.6	-4.0
$\text{PDE}_{(\text{Eupa}^{+\bullet} \rightarrow \text{Eupa}(-5\text{H})^\bullet + \text{H}^+)}$	241.2	41.4	18.3	22.5
$\text{PDG}_{(\text{Eupa}^{+\bullet} \rightarrow \text{Eupa}(-7\text{H})^\bullet + \text{H}^+)}$	228.2	33.9	10.1	-4.3
$\text{PDE}_{(\text{Eupa}^{+\bullet} \rightarrow \text{Eupa}(-7\text{H})^\bullet + \text{H}^+)}$	235.9	37.0	17.0	21.5

cation form ($\text{Eupa}^{+\bullet}$) converted from the eupatilin in polar environments. This is the reason why the single electron transfer process from eupatilin to hydroxyl radical is favored in the polar solvent. Our calculations agree with the results reported previously.^[44] The radical cation form of eupatilin in the polar solvents is about 50 kcal/mol more stable than in nonpolar one, and the OH^- is about 30 kcal/mol more stable in the polar solvents than in nonpolar one, which eventually results in the negative, exergonic values of $\Delta_r G$ in the two polar solvents.

The second step of SEPT mechanism is the proton dissociation process ($\text{Eupa}^{+\bullet} \rightarrow \text{Eupa}(-\text{H})^\bullet + \text{H}^+$, proton dissociation Gibbs free energy (PDG)). The proton dissociation Gibbs free energies in the studied solutions are significantly lower than that in gas phase due to the large solvation Gibbs free energies of proton. The calculated PDG values in water, methanol, and benzene are 37.6, 10.6, and -4.0 kcal/mol for the formation of $\text{Eupa}(-5\text{H})^\bullet$ and the values are 33.9, 10.1, and -4.3 kcal/mol for the formation of $\text{Eupa}(-7\text{H})^\bullet$ in the proton dissociation process. The gas phase values reaches 232.7 and 228.2 kcal/mol for the formation of $\text{Eupa}(-5\text{H})^\bullet$ and $\text{Eupa}(-7\text{H})^\bullet$, respectively. As observed, the proton dissociation process is thermodynamically favored only in aqueous medium. PDG increases in the same order as the IPGs and $\Delta_r G$ of the first step: water < methanol < benzene < gas phase.

Enthalpy Changes The reaction enthalpies in electron transfer process ($\text{Eupa} + \text{OH}^\bullet \rightarrow \text{Eupa}^{+\bullet} + \text{OH}^-$, $\Delta_r H$) are endothermic in gas and benzene environment, with $\Delta_r H = -0.2$ and -2.9 kcal/mol. The data are exothermic in methanol and water solutions, with the value of $\Delta_r H = 125.8$ and 63.4 kcal/mol. The rel-

Table 3. Half reaction enthalpy (IP, EA) and Gibbs free energy (IPG, EG, in kcal/mol) at 298.15 K for SEPT in gas phase, benzene, methanol, and water solutions ($\text{Eupa} \rightarrow \text{Eupa}^{+\bullet} + \text{e}^-$ and $\text{OH}^\bullet + \text{e}^- \rightarrow \text{OH}^-$).

	Gas	Benzene	Methanol	Water
$\text{IPG}_{(\text{Eupa} \rightarrow \text{Eupa}^{+\bullet} + \text{e}^-)}$	165.9	149.9	117.4	98.3
$\text{IP}_{(\text{Eupa} \rightarrow \text{Eupa}^{+\bullet} + \text{e}^-)}$	167.5	150.1	115.5	110.3
$\text{EG}_{(\text{OH}^\bullet + \text{e}^- \rightarrow \text{OH}^-)}$	-40.5	-86.9	-118.0	-101.7
$\text{EAG}_{(\text{OH}^\bullet + \text{e}^- \rightarrow \text{OH}^-)}$	-41.7	-86.7	-115.7	-113.2

ative order of reaction enthalpies in the studied environments is water < methanol < benzene < gas, which agrees with the order of reaction Gibbs free energies. In the first step, one half reaction, the electron transfer from the neutral form ($\text{Eupa} \rightarrow \text{Eupa}^{+\bullet} + \text{e}^-$, ionization potentials (IP)) is endothermic independent of the polarity of solvents. The relative IPs order is water < methanol < benzene < gas, which is in agreement with the result reported by Rimarcik et al.^[55] The electron donation ability of eupatilin is comparable to α -tocopherol, quercetin, and kaempferol, stronger than that of cyanidin, phenols, tetracyano-p-phenylenediamine and some substituted chromans.^[42,55,59-63] The other half reaction, the electron transfer from the hydroxyl radical ($\text{OH}^\bullet + \text{e}^- \rightarrow \text{OH}^-$, electron affinity (EA)) is exothermic in the studied environments. The OH^- is about 30 kcal/mol more stable in the polar solvents than in nonpolar one. The solvation contributions of the polar solvents lead to the negative reaction enthalpy values of $\Delta_r H$ in the two polar solvents.

In the next step, proton dissociation process ($\text{Eupa}^{+\bullet} \rightarrow \text{Eupa}(-\text{H})^\bullet + \text{H}^+$, proton dissociation enthalpy (PDE)), the calculated PDEs for the formation of $\text{Eupa}(-5\text{H})^\bullet$ in benzene, methanol, and water are 41.4, 18.3, and 22.5 kcal/mol, respectively. The gas phase value reaches 241.2 kcal/mol. For the formation of $\text{Eupa}(-7\text{H})^\bullet$ in the proton dissociation process, the predicted PDE values in benzene, methanol, and water are 37.0, 17.0, and 21.5 kcal/mol, respectively. The gas phase value reaches 235.9 kcal/mol. The high solvation enthalpies of proton decrease the PDE value in solution significantly. The difference between water and gas phase reaches ~220 kcal/mol. PDEs increase in the order: methanol < water < benzene < gas phase. Our results are consistent with the conclusions reported by Rimarcik et al.^[55] Furthermore, the proton dissociation ability of eupatilin is comparable to that of α -tocopherol, chroman-6-ol, and chroman-6-ol analogs with electron-donating substituents.^[42,59-61]

able to that of α -tocopherol, chroman-6-ol, and chroman-6-ol analogs with electron-donating substituents.^[42,59-61]

Sequential proton loss electron transfer

In the SPLET mechanism, the first step is the proton dissociation process from eupatilin to anionic form ($\text{Eupa} \rightarrow \text{Eupa}(-\text{H})^- + \text{H}^+$). The next step is single electron transfer from anionic form of eupatilin to hydroxyl radical ($\text{Eupa}(-\text{H})^- + \text{OH}^\bullet \rightarrow \text{Eupa}(-\text{H})^\bullet + \text{OH}^-$). The reaction Gibbs free energies and enthalpies for two steps are reported in Table 4. The

Table 4. Reaction enthalpy and Gibbs free energy (in kcal/mol) at 298.15 K for SPLET mechanism in gas phase, benzene, methanol, and water solutions ($\text{Eupa} \rightarrow \text{Eupa}(-\text{H})^- + \text{H}^+$ and $\text{Eupa}(-\text{H})^- + \text{OH}^\bullet \rightarrow \text{Eupa}(-\text{H})^\bullet + \text{OH}^-$).

	Gas	Benzene	Methanol	Water
$\text{PAG}_{(\text{Eupa} \rightarrow \text{Eupa}(-5\text{H})^- + \text{H}^+)}$	337.5	104.8	41.2	24.8
$\text{PA}_{(\text{Eupa} \rightarrow \text{Eupa}(-5\text{H})^- + \text{H}^+)}$	346.0	108.6	48.9	51.4
$\text{PAG}_{(\text{Eupa} \rightarrow \text{Eupa}(-7\text{H})^- + \text{H}^+)}$	325.3	93.7	33.5	17.4
$\text{PA}_{(\text{Eupa} \rightarrow \text{Eupa}(-7\text{H})^- + \text{H}^+)}$	333.5	97.2	40.9	43.7
$\Delta_r G_{(\text{Eupa}(-5\text{H})^- + \text{OH}^\bullet \rightarrow \text{Eupa}(-5\text{H})^\bullet + \text{OH}^-)}$	20.6	-4.3	-31.2	-32.1
$\Delta_r H_{(\text{Eupa}(-5\text{H})^- + \text{OH}^\bullet \rightarrow \text{Eupa}(-5\text{H})^\bullet + \text{OH}^-)}$	21.0	-3.9	-30.8	-31.7
$\Delta_r G_{(\text{Eupa}(-7\text{H})^- + \text{OH}^\bullet \rightarrow \text{Eupa}(-7\text{H})^\bullet + \text{OH}^-)}$	28.3	3.2	-24.0	-25.0
$\Delta_r H_{(\text{Eupa}(-7\text{H})^- + \text{OH}^\bullet \rightarrow \text{Eupa}(-7\text{H})^\bullet + \text{OH}^-)}$	28.2	3.1	-24.1	-25.1

Table 5. Half reaction enthalpy (ETE) and Gibbs free energy (ETG, in kcal/mol) at 298.15 K for SEPT in gas phase, benzene, methanol, and water solutions ($\text{Eupa}(-\text{H})^- \rightarrow \text{Eupa}(-\text{H})^\bullet + \text{e}^-$).

	Gas	Benzene	Methanol	Water
ETG _{(Eupa(-5H)⁻→Eupa(-5H)[•]+e⁻)}	61.2	82.6	86.8	69.5
ETE _{(Eupa(-5H)⁻→Eupa(-5H)[•]+e⁻)}	62.7	82.9	84.9	81.5
ETG _{(Eupa(-7H)⁻→Eupa(-7H)[•]+e⁻)}	68.8	90.1	94.0	76.7
ETE _{(Eupa(-7H)⁻→Eupa(-7H)[•]+e⁻)}	69.9	89.9	91.6	88.2

half reaction Gibbs free energy (electron transfer Gibbs free energy (ETG)) and enthalpies (electron transfer enthalpy (ETE)) of the electron transfer process in the first step ($\text{Eupa}(-\text{H})^- \rightarrow \text{Eupa}(-\text{H})^\bullet + \text{e}^-$), are listed in Table 5.

Gibbs Free Energy Changes In the first step ($\text{Eupa} \rightarrow \text{Eupa}(-\text{H})^- + \text{H}^+$, PAG), the proton loss from eupatilin is found to be endergonic, regardless of the polarity of the environment. Because of high solvation Gibbs free energies of proton, proton affinity Gibbs free energy (PAGs) in the studied solutions is significantly lower than corresponding gas phase value for the formation of two anionic form ($\text{Eupa}(-5\text{H})^-$ and $\text{Eupa}(-7\text{H})^-$). The proton dissociation Gibbs free energies in the studied environment increase in the order of water < methanol < benzene < gas. The PAG values for the formation of $\text{Eupa}(-5\text{H})^-$ in benzene, methanol, and water are 104.8, 41.2, and 24.8 kcal/mol, respectively. The corresponding value in gas phase reaches 337.5 kcal/mol. For the formation of $\text{Eupa}(-7\text{H})^-$ in benzene, methanol, and water, the PAG values are 93.7, 33.5, and 17.4 kcal/mol, respectively. The gas phase value reaches 325.3 kcal/mol.

The next step is single electron transfer process ($\text{Eupa}(-\text{H})^- + \text{OH}^\bullet \rightarrow \text{Eupa}(-\text{H})^\bullet + \text{OH}^-$, $\Delta_r G$). It can be seen from Table 4 that the second step is exergonic for the formation of $\text{Eupa}(-5\text{H})^\bullet$ and $\text{Eupa}(-7\text{H})^\bullet$ in the two polar solvents, methanol and water. The values for the formation of $\text{Eupa}(-5\text{H})^\bullet$ in methanol and water are -31.2 and -32.1 kcal/mol, respectively. The corresponding values for the formation of $\text{Eupa}(-5\text{H})^\bullet$ are -24.0 and -25.0 kcal/mol, respectively in methanol and water. In benzene, the process is thermodynamically favored for the formation of $\text{Eupa}(-5\text{H})^\bullet$, with $\Delta_r G = -4.3$ kcal/mol. However, the process in benzene is thermodynamically forbidden for the formation of $\text{Eupa}(-7\text{H})^\bullet$, with $\Delta_r G = 3.2$ kcal/mol. In gas phase, the process is thermodynamically forbidden for the formation of $\text{Eupa}(-5\text{H})^\bullet$ and $\text{Eupa}(-7\text{H})^\bullet$. The corresponding values are 21.0 and 28.2 kcal/mol for formation of $\text{Eupa}(-5\text{H})^\bullet$ or $\text{Eupa}(-7\text{H})^\bullet$, respectively. Larger exergonicities are found for the formation of $\text{Eupa}(-7\text{H})^\bullet$. The data increase in the order of: water < methanol < benzene < gas, which agree with the result reported by Rimarcik et al.^[55] Furthermore, $\Delta_r G$ s of the electron transfer from the neutral form are about 20 kcal/mol greater than that from the anionic form in the studied environments. Accordingly, single electron transfer process from the anionic form is more preferable than that from the neutral form, which is consistent with the results obtained by other studies.^[32,33,35,58,64]

In the half reaction of the second step, the electron transfer from anionic form ($\text{Eupa}(-\text{H})^- - \text{e}^- \rightarrow \text{Eupa}(-\text{H})^\bullet$, ETE) is found to be endergonic, regardless of the polarity of the environment. The data decrease in the order of: methanol > benzene > water > gas, which is in agreement with the sequence of corresponding enthalpic changes reported by Rimarcik et al.^[55] The ETGs of $\text{Eupa}(-5\text{H})^- - \text{e}^- \rightarrow \text{Eupa}(-5\text{H})^\bullet$ are about 7 kcal/mol lower than that of $\text{Eupa}(-7\text{H})^- - \text{e}^- \rightarrow \text{Eupa}(-7\text{H})^\bullet$ in the studied environments, which result in the thermodynamically preferred for the former process. In addition, Tables 3 and 4 clearly show that the differences between IPGs and ETGs exceed 30 kcal/mol. Thus, the electron donation ability of anionic form is stronger than that of neutral form.

Enthalpy Changes The enthalpic changes of proton loss process ($\text{Eupa} \rightarrow \text{Eupa}(-\text{H})^- + \text{H}^+$, PA) in solutions are significantly lower than those in gas phase due to the large solvation enthalpies of proton. The proton affinity (PA) values for the formation of $\text{Eupa}(-5\text{H})^-$ are 108.6, 48.9, and 51.4 kcal/mol, respectively, in benzene, methanol, and water. They are significantly lower than corresponding gas phase value (346.0 kcal/mol). For the formation of $\text{Eupa}(-7\text{H})^-$, the values in gas, benzene, methanol, and water are 333.5, 97.2, 40.9, and 43.7 kcal/mol, respectively. The differences between gas phase and water exceed 285 kcal/mol. The relative order of PAs is methanol < water < benzene < gas, which is consistent with the result by Rimarcik et al.^[55] As observed, formation of $\text{Eupa}(-5\text{H})^-$ is easier than formation of $\text{Eupa}(-7\text{H})^-$. The proton donation ability of eupatilin is comparable to α -tocopherol, and even stronger than that of p-phenylenediamines, tetracyano-p-phenylenediamine, chroman-6-ol, and some chroman-6-ol analogs.^[42,55,59-63]

The reaction enthalpies of the second step ($\text{Eupa}(-\text{H})^- + \text{OH}^\bullet \rightarrow \text{Eupa}(-\text{H})^\bullet + \text{OH}^-$, $\Delta_r H$) are exothermic in benzene, methanol, and water for the formation of $\text{Eupa}(-5\text{H})^\bullet$, with the values of $\Delta_r H = -3.9$, -30.8, and -31.7 kcal/mol, respectively. For the formation of $\text{Eupa}(-7\text{H})^\bullet$, the process is exothermic in methanol and water, with $\Delta_r H = -24.0$ and -25.0 kcal/mol, respectively. The sequence of $\Delta_r H$ in the studied solvents is water < methanol < benzene < gas, which is in agreement with the sequence of corresponding Gibbs free energies.

In the half reaction of the second step ($\text{Eupa}(-\text{H})^- - \text{e}^- \rightarrow \text{Eupa}(-\text{H})^\bullet$, ETE), the enthalpy changes are endothermic in the studied solvents. The relative order of ETEs is methanol > benzene > water > gas, which is consistent with the sequence of corresponding enthalpic changes reported by Rimarcik et al.^[55] The ETEs of $\text{Eupa}(-5\text{H})^- - \text{e}^- \rightarrow \text{Eupa}(-5\text{H})^\bullet$ are lower than those of $\text{Eupa}(-7\text{H})^- - \text{e}^- \rightarrow \text{Eupa}(-7\text{H})^\bullet$ in the studied solvents. Thus, the formation of $\text{Eupa}(-5\text{H})^\bullet$ is more preferable than formation of $\text{Eupa}(-7\text{H})^\bullet$. In addition, ETEs are lower than IPs. Accordingly, the electron donation ability of the anionic form is stronger than the neutral form. The electron donation ability of the anionic form of eupatilin is much weaker than α -tocopherol, chroman-6-ol, and chroman-6-ol analogs, and stronger than that of phenol and tetracyano-p-phenylenediamine.^[42,55,59-63]

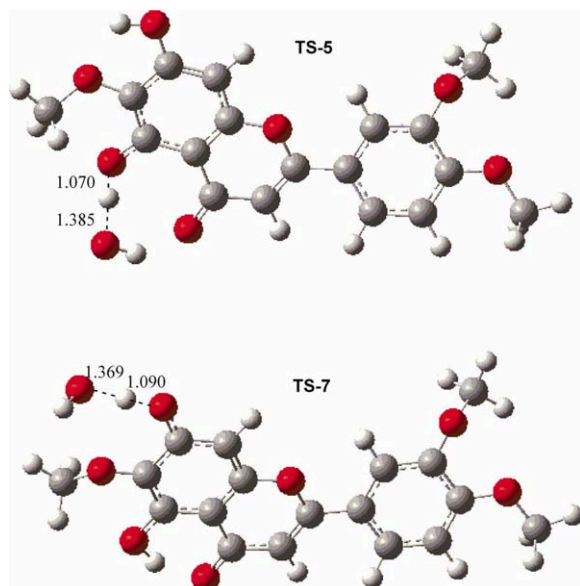


Figure 3. Optimized geometries of the transition states corresponding to HA mechanism (in Å). [Color figure can be viewed in the online issue, which is available at wileyonlinelibrary.com.]

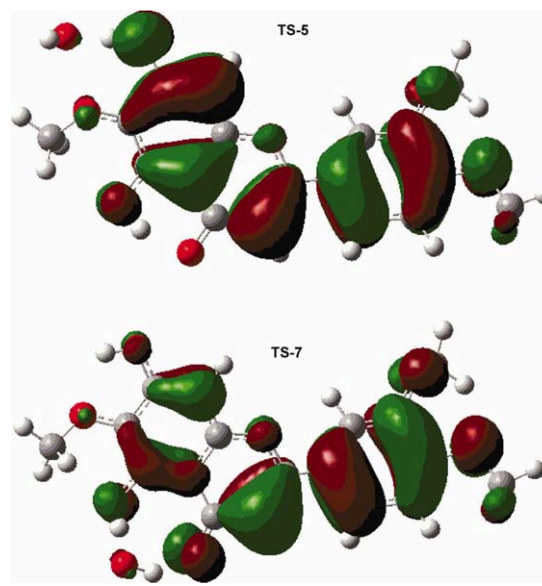


Figure 4. SOMO density surfaces of the HA transition state structures. [Color figure can be viewed in the online issue, which is available at wileyonlinelibrary.com.]

Hydrogen abstraction mechanisms

Analysis of Spin Densities, NBO Charges, and SOMO HA reaction by OH[•] may be divided into two types. On one hand, the radicals abstract a hydrogen atom from eupatilin through the HAT mechanism. In this mechanism, the radical nature would be transferred to eupatilin. On the other hand, the proton and the electron are progressively and simultaneously transferred from Eupa to OH[•] through PCET mechanism. Both HAT and PCET yield the same products, Eupa radical.^[6,34,35,65] To get insight into the HA mechanism, we have systematically calculated the optimized geometries and energies of the reactants, transition states (TSs), and products for all possible HAs from 5 and 7 hydroxyl groups. The optimized geometries of the transition states are shown in Fig. 3. In the HA mechanism, partial detachment of H atom from OH group is observed in the transition state. The distance between the atoms involved in the abstractions (O—H) in transition states increase with respect to corresponding bonds in eupatilin (0.978 and 1.00 Å).

The spin density and charge of the reactants, transition states, and products obtained from natural population analysis calculations are reported in Table 6. For two TS structures, the spin populations are found to be concentrated on the eupatilin(—H) and OH[•], and a much small negative value is found on the transferred hydrogen. In addition, the spin densities associated to the eupatilin(—H) in two TSs is increased, whereas that of hydroxyl radical is decreased in comparison to the reactants. Moreover, the transferred hydrogen with substantial positive charge is typical for proton migrations.^[35,66,67,68] These data indicate that the electron and the proton are moving in the same direction from eupatilin to hydroxyl radical in the reaction of eupatilin with OH[•], which corresponds to PCET but not HAT mechanism.

The SOMO of two transition states (TS5 and TS7, Fig. 4) reveals that the unpaired electron is mainly delocalized on the eupatilin(—H) fragment, including the oxygen atom where deprotonation takes place. The electron densities in atomic orbitals are orthogonal to, but not along, the transition vector

Table 6. Atomic spin densities and NBO charges of reactants, TSs, and products from nature orbital population analysis.

		Spin density			NBO charge		
		Benzene	Methanol	Water	Benzene	Methanol	Water
Reactants	Eupa	0	0	0	0	0	0
	OH [•]	1	1	1	0	0	0
TS-5	Eupa(—H)	0.447	0.671	0.688	−0.205	0.000	0.016
	<i>H</i> _{transfer}	−0.028	−0.026	−0.025	0.469	0.475	0.476
	OH	0.581	0.355	0.337	−0.264	−0.476	−0.492
TS-7	Eupa(—H)	0.525	0.621	0.630	−0.153	−0.065	−0.056
	<i>H</i> _{transfer}	−0.009	−0.008	−0.008	0.485	0.487	0.487
	OH	0.484	0.387	0.378	−0.332	−0.422	−0.431
Products	Eupa(—H) [•]	1	1	1	0	0	0
	H ₂ O	0	0	0	0	0	0

Table 7. Reaction enthalpies and Gibbs free energies ($\Delta_r H$ and $\Delta_r G$), Gibbs free energies of activation ($\Delta_r G^\ddagger$), in kcal/mol, and the ratio of products at 298.15 K for the HA reactions of Eupa with OH^\bullet in gas phase, benzene, methanol, and water solutions. ($\text{Eupa} + \text{OH}^\bullet \rightarrow \text{Eupa}(-\text{H})^\bullet + \text{H}_2\text{O}$).

	Gas	Benzene	Methanol	Water
$\Delta_r G^\ddagger_{(\text{Eupa}+\text{OH}^\bullet \rightarrow [\text{Eupa}(-5\text{H})\cdots\text{H}\cdots\text{OH}]^\ddagger)}$	10.1	10.6	11.2	11.2
$\Delta_r G_{(\text{Eupa}+\text{OH}^\bullet \rightarrow \text{Eupa}(-5\text{H})^\bullet + \text{H}_2\text{O})}$	-24.2	-26.3	-31.4	-31.7
$\Delta_r H_{(\text{Eupa}+\text{OH}^\bullet \rightarrow \text{Eupa}(-5\text{H})^\bullet + \text{H}_2\text{O})}$	-22.0	-24.0	-29.2	-29.4
$\Delta_r G^\ddagger_{(\text{Eupa}+\text{OH}^\bullet \rightarrow [\text{Eupa}(-7\text{H})\cdots\text{H}\cdots\text{OH}]^\ddagger)}$	2.1	3.0	6.0	6.3
$\Delta_r G_{(\text{Eupa}+\text{OH}^\bullet \rightarrow \text{Eupa}(-7\text{H})^\bullet + \text{H}_2\text{O})}$	-28.8	-29.9	-32.0	-31.9
$\Delta_r H_{(\text{Eupa}+\text{OH}^\bullet \rightarrow \text{Eupa}(-7\text{H})^\bullet + \text{H}_2\text{O})}$	-27.3	-28.4	-30.5	-30.4
Ratio $\left(\frac{[\text{Eupa}(-5\text{H})^\bullet]}{[\text{Eupa}(-7\text{H})^\bullet]}\right)$	1.4×10^{-6}	2.7×10^{-6}	1.5×10^{-4}	2.6×10^{-4}

(donor-H-acceptor). It is commonly believed that the SOMO of HAT TSs should have significant density in atomic orbitals oriented along or nearly along the transition vector. The SOMO of PCET TSs, however, involves p orbitals that are orthogonal to the vector.^[34,66,68] The SOMO of TS-5 and TS-7 is consistent with PCET transition states. Dhaouadi et al.^[6] recently reported that the HA mechanism for the reaction of quercetin with hydroxyl radical is also governed by PCET mechanism in gas phase.

Gibbs Free Energy Changes The Gibbs free energies of reactions ($\Delta_r G$) and barriers ($\Delta_r G^\ddagger$) for HA mechanism ($\text{Eupa} + \text{OH}^\bullet \rightarrow \text{Eupa}(-\text{H})^\bullet + \text{H}_2\text{O}$) are reported in Table 7. As observed, OH^\bullet can abstract H atom from two different sites. The Gibbs free energies for the abstraction reaction from position 7 are lower than that from position 5. The attack of the radical takes place preferentially at position H7, with $\Delta_r G$ around -30 kcal/mol in different environments. In addition, the activation energies ($\Delta_r G^\ddagger$) for the reaction from position 7 are also lower than that from position 5. According to the Curtin-Hammond principle, the distribution of the products is determined by the difference of activation energies $\left(\frac{p_1}{p_2} = e^{-\frac{\Delta G_1^\ddagger - \Delta G_2^\ddagger}{RT}}\right)$.^[69] The resulting ratios between the concentrations of products are also given in Table 7. The main product is $\text{Eupa}(-7\text{H})^\bullet$ regardless of the environments.

The half reaction is bond dissociation process ($\text{Eupa} \rightarrow \text{Eupa}(-\text{H})^\bullet + \text{H}^\bullet$, bond dissociation Gibbs free energy (BDG)). The BDGs are reported in Table 8. As observed, the values of BDG are in 77 and 84 kcal/mol range. The values for the abstraction from position 7 are lower than those from position 5 in different environments, which suggests that H at position 7 is more preferably abstracted than H at position 5 in ther-

modynamics. In the studied environments, the order of the BDG is water < methanol < benzene < gas.

Enthalpy Changes The reaction enthalpies for HA mechanism ($\text{Eupa} + \text{OH}^\bullet \rightarrow \text{Eupa}(-\text{H})^\bullet + \text{H}_2\text{O}$, $\Delta_r H$) are reported in Table 7. The reaction enthalpies are around -27 kcal/mol in different environments. The HA process is exothermic in the studied environments. Furthermore, the reaction enthalpies from position 7 are lower than those from position 5. The order of the reaction enthalpies is water < methanol < benzene < gas.

The bond dissociation enthalpies of the half reaction ($\text{Eupa} \rightarrow \text{Eupa}(-\text{H})^\bullet + \text{H}^\bullet$, bond dissociation enthalpy (BDE)) are listed in Table 8. Table 8 clearly shows that the BDE is in 86–94 kcal/mol range. The values for $\text{Eupa} \rightarrow \text{Eupa}(-7\text{H})^\bullet + \text{H}^\bullet$ are around 5 kcal/mol lower than that for $\text{Eupa} \rightarrow \text{Eupa}(-5\text{H})^\bullet + \text{H}^\bullet$, which also show that H-atom at position 7 is more preferably abstracted than that at position 5 in thermodynamics. In the studied environments, the sequence of the BDE is water \approx methanol < benzene < gas. The H-atom donation ability of eupatilin is stronger than that of phenol, phenol analogs and a few flavonoids such as apigenin and lysionotin but weaker than that of α -tocopherol, chroman analogs, thiophenols derivatives, and flavonoids such as quercetin, morin, myricetin, luteolin, kaempferol, and baicalein.^[6,42,55,59–63]

Thermodynamically favored mechanism

To study the antioxidant mechanism of eupatilin, we calculate the reaction Gibbs free energies and enthalpies, and the half reaction Gibbs free energies and enthalpies of SEPT, SPLET, and HA mechanisms. For the half reaction of eupatilin, as above discussed, the electron transfer process in SEPT and SPLET mechanism is thermodynamically forbidden in gas, benzene, methanol, and water. Likewise, the bond dissociation process is thermodynamically unfavored in HA mechanism.

For the reaction of eupatilin with OH radical, the two steps of the SEPT mechanism are favored in water. Obviously, the SEPT is thermodynamically favored mechanism in water. For the SPLET mechanism, the first step of proton loss process is forbidden in the studied environments. Once the anionic form formed, the second step of electron transfer process is favored in methanol and water. HA process with negative $\Delta_r G$ in the studied environment exhibits that HA is thermodynamically favored mechanism independent of the polarity of solvents.

Table 8. Half reaction enthalpy (BDE) and Gibbs free energy (BDG in kcal/mol) at 298.15 K for the HA process in Gas phase, benzene, methanol and water solutions ($\text{Eupa} \rightarrow \text{Eupa}(-\text{H})^\bullet + \text{H}^\bullet$).

	Gas	Benzene	Methanol	Water
BDG ($\text{Eupa} \rightarrow \text{Eupa}(-5\text{H})^\bullet + \text{H}^\bullet$)	83.8	82.0	77.6	77.4
BDE ($\text{Eupa} \rightarrow \text{Eupa}(-5\text{H})^\bullet + \text{H}^\bullet$)	93.5	91.7	87.3	87.1
BDG ($\text{Eupa} \rightarrow \text{Eupa}(-7\text{H})^\bullet + \text{H}^\bullet$)	79.3	78.4	77.0	77.1
BDE ($\text{Eupa} \rightarrow \text{Eupa}(-7\text{H})^\bullet + \text{H}^\bullet$)	88.2	87.3	86.0	86.0

The reaction of eupatilin with hydroxyl radical is more energetically favorable to occur in a more polar solvent.

Conclusions

In this work, the reaction of eupatilin with OH radical in gas phase and solution has been studied using the density functional theory (DFT) at the B3LYP/6-311++g(2df,2p)//B3LYP/6-31g(d) level and the PCM to account for solvent effects. Different mechanisms and reaction sites have been considered. The SEPT mechanism is thermodynamically favored in water. Once the anionic form is produced, the second step in SPLET mechanism is thermodynamically favored in methanol and water. The HA is thermodynamically favored mechanism in gas, benzene, methanol, and water. The analysis of the NBO spin densities and charges as well as the SOMO of TS indicates that the HA process is governed by PCET mechanism. The main product is eupatilin(−7H) radical according to the Curtin–Hammond principle. In addition, the HA and SEPT mechanisms are more energetically favorable than the SPLET mechanism and they are all more preferable to occur in more polar solvent in thermodynamics.

Keywords: eupatilin • density functional theory • radical scavenging mechanisms • hydroxyl radical

How to cite this article: M. Li, W. Liu, C. Peng, Q. Ren, W. Lu, W. Deng, *Int. J. Quantum Chem.* **2013**, *113*, 966–974. DOI: 10.1002/qua.24060.

- [1] H. Kamiya, T. Ueda, T. Ohgil, A. H. Kasai, *Nucleic Acids Res.* **1995**, *23*, 761.
- [2] A. Jenner, T. G. England, O. I. Aruoma, B. Halliwell, *Biochem. J.* **1998**, *331*, 365.
- [3] V. Y. Antonchenko, E. J. Kryachko, *Phys. Chem. A* **2005**, *109*, 3052.
- [4] A. Agarwal, S. Gupta, L. Sekhon, R. Shah, *Antioxid. Redox Signalling* **2008**, *10*, 1375.
- [5] (a) W. R. Markesbery, J. M. Carney, *Brain Pathol.* **1999**, *9*, 133; (b) M. F. Beal, *Free Radical Biol. Med.* **2002**, *32*, 797.
- [6] Z. Dhaouadi, M. Nsangou, N. Garrab, E. H. Anouar, K. Marakchi, S. Lahmar, *J. Mol. Struct.: Theochem.* **2009**, *904*, 35.
- [7] S. E. Browne, M. F. Beal, *Antioxid. Redox Signalling* **2006**, *8*, 2061.
- [8] M. Aslan, T. Ozben, *Curr. Alzheimer Res.* **2004**, *1*, 111.
- [9] C. Behl, *Subcell. Biochem.* **2005**, *38*, 65.
- [10] P. Jenner, *Ann. Neurol.* **2003**, *53*, S26.
- [11] G. Appendino, O. Tagliatela-Scafati, A. Romano, F. Pollastro, C. Avonto, P. Rubiolo, *J. Nat. Prod.* **2009**, *73*, 340.
- [12] G. Appendino, F. Belliardo, G. M. Nano, S. Stefanelli, *J. Agric. Food Chem.* **1982**, *30*, 518.
- [13] E. J. Choi, H. M. Oh, B. R. Na, T. P. Ramesh, H. J. Lee, C. S. Choi, S. C. Choi, T. Y. Oh, S. J. Choi, J. R. Chae, S. W. Kim, C. D. Jun, *Pharm. Res.* **2008**, *25*, 1355.
- [14] S. Lee, M. Lee, S. H. Kim, *Food Chem. Toxicol.* **2008**, *46*, 2865.
- [15] E. J. Choi, H. M. Oh, H. Wee, C. S. Choi, S. C. Choi, K. H. Kim, W. C. Han, T. Y. Oh, S. H. Kim, C. D. Jun, *Differentiation* **2009**, *77*, 412.
- [16] A. Giangaspero, C. Ponti, F. Pollastro, G. D. Favero, R. D. Loggia, A. Tubaro, G. Appendino, S. Sosa, *J. Agric. Food Chem.* **2009**, *57*, 7726.
- [17] H. Y. Ji, S. Y. Kim, D. K. Kim, J. H. Joong, H. S. Lee, *Molecules* **2010**, *15*, 6466.
- [18] M. J. Kim, M. H. Park, M. K. Jeong, J. D. Yeo, W. I. Cho, P. S. Chang, J. H. Chung, J. H. Lee, *Food Sci. Biotechnol.* **2010**, *19*, 535.
- [19] M. J. Kim, D. H. Kim, H. K. Na, Y. Surh, *J. Biochem. Pharmacol.* **2010**, *80*, 2092.
- [20] J. H. Cho, J. G. Lee, Y. I. Yang, J. H. Kim, J. H. Ahn, N. I. Baek, K. T. Lee, J. H. Choi, *Food Chem. Toxicol.* **2011**, *49*, 1737.
- [21] K. D. Yoon, Y. W. Chin, M. H. Yang, J. Kim, *Food Chem.* **2011**, *129*, 679.
- [22] E. J. Choi, S. Lee, J. R. Chae, H. S. Lee, C. D. Jun, S. H. Kim, *Life Sci.* **2011**, *88*, 1121.
- [23] T. Nakasugi, M. Nakashima, K. Komai, *J. Agric. Food Chem.* **2000**, *48*, 3256.
- [24] I. Nakanishi, T. Kawashima, K. Ohkubo, H. Kanazawa, K. Inami, M. Mochizuki, S. Fukuzumi, N. Ikota, *Org. Biomol. Chem.* **2005**, *3*, 626.
- [25] M. Musialik, G. Litwinienko, *Org. Lett.* **2005**, *7*, 4951.
- [26] L. Estevez, R. A. Mosquera, *J. Phys. Chem. A* **2008**, *112*, 10614.
- [27] H. Y. Zhang, Y. M. Sun, X. L. Wang, *Chem. Eur. J.* **2003**, *9*, 502.
- [28] H. Y. Zhang, H. F. Ji, *New J. Chem.* **2006**, *30*, 503.
- [29] L. Shen, H. Y. Zhang, H. F. Ji, *Org. Lett.* **2005**, *7*, 243.
- [30] J. S. Wright, D. J. Carpenter, D. J. McKay, K. U. Ingold, *J. Am. Chem. Soc.* **1997**, *119*, 4245.
- [31] (a) M.-J. Li, L. Liu, Y. Fu, Q.-X. Guo, *Theochem* **2007**, *815*, 1; (b) M.-J. Li, Y. Fu, H.-J. Wang, Y.-Q. Li, L. Liu, Q.-X. Guo, *Acta Chim. Sin.* **2007**, *65*, 1243; (c) Y. Fu, L. Liu, Y. Mou, B.-L. Lin, Q.-X. Guo, *Theochem* **2004**, *674*, 241.
- [32] (a) M. J. Li, Y. J. Li, C. R. Peng, W. C. Lu, *Acta Phys. Chim. Sin.* **2010**, *26*, 466; (b) M. J. Li, L. M. Zhang, W. X. Liu, W. C. Lu, *Chin. J. Chem. Phys.* **2011**, *24*, 173.
- [33] M. Francisco-Marquez, A. Galano, *J. Phys. Chem. B* **2009**, *113*, 16077.
- [34] A. Galano, N. A. Macías-Ruvalcaba, O. N. M. Campos, J. Pedraza-Chaverri, *J. Phys. Chem. B* **2010**, *114*, 6625.
- [35] A. Pérez-González, A. Galano, *J. Phys. Chem. B* **2011**, *115*, 1306.
- [36] M. J. Frisch, G. W. Trucks, H. B. Schlegel, Gaussian 03, Revision C.02; Gaussian: Wallingford, CT, **2004**.
- [37] (a) A. D. Becke, *J. Chem. Phys.* **1993**, *98*, 5648; (b) C. Lee, W. Yang, R. G. Parr, *Phys. Rev. B* **1988**, *37*, 785.
- [38] (a) M. S. Gordon, *Chem. Phys. Lett.* **1980**, *76*, 163; (b) T. Clark, J. Chandrasekhar, G. W. Spitznagel, P. v. R. Schleyer, *J. Comp. Chem.* **1983**, *4*, 294.
- [39] J. M. Matxain, M. Ristilä, A. Strid, L. A. Eriksson, *Chem. Eur. J.* **2007**, *13*, 4636.
- [40] N. Nenadis, M. P. Sigalas, *J. Phys. Chem. A* **2008**, *112*, 12196.
- [41] J. M. Matxain, D. Padro, M. Ristilä, A. Strid, L. A. Eriksson, *J. Phys. Chem. B* **2009**, *113*, 9629.
- [42] M. Najafi, K. H. Mood, M. Zahedi, E. Klein, *Comput. Theor. Chem.* **2011**, *969*, 1.
- [43] R. F. Jin, H. Z. Bao, *Int. J. Quantum Chem.* **2011**, *111*, 1064.
- [44] J. P. Cerón-Carrasco, A. Bastida, A. Requena, J. Zúñiga, *J. Phys. Chem. B* **2010**, *114*, 4366.
- [45] J. Tomasi, B. Mennucci, R. Cammi, *Chem. Rev.* **2005**, *105*, 2999.
- [46] V. Barone, M. Cossi, J. Tomasi, *J. Chem. Phys.* **1997**, *107*, 3210.
- [47] (a) Y. Fu, L. Liu, R.-Q. Li, R. Liu, Q.-X. Guo, *J. Am. Chem. Soc.* **2004**, *126*, 814; (b) Y. Fu, L. Liu, H. Z. Yu, Y.-M. Wang, Q.-X. Guo, *J. Am. Chem. Soc.* **2005**, *127*, 7227; (c) Y. Fu, L. Liu, Y.-M. Wang, J.-N. Li, T.-Q. Yu, Q.-X. Guo, *J. Phys. Chem. A* **2006**, *110*, 5874; (d) Y. Fu, K. Shen, L. Liu, Q.-X. Guo, *J. Am. Chem. Soc.* **2007**, *129*, 13510.
- [48] E. D. Glendenning, J. K. Badenhoop, A. E. Reed, J. E. Carpenter, J. A. Bohmann, C. M. Morales, F. Weinhold, NBO Version 5.0, Theoretical Chemistry Institute, University of Wisconsin, Madison, **2001**.
- [49] (a) H. Y. Zhang, H. F. Ji, *J. Mol. Struct.: Theochem.* **2003**, *663*, 167; (b) A. K. Chandra, T. Uchimar, *Int. J. Mol. Sci.* **2002**, *3*, 407.
- [50] M.-J. Li, L. Liu, Y. Fu, Q.-X. Guo, *J. Phys. Chem. B* **2005**, *109*, 13818.
- [51] F. Bohr, E. Henon, *J. Phys. Chem. A* **1998**, *102*, 4857.
- [52] M. M. Bizarro, B. J. C. Cabral, R. M. B. dos Santos, J. A. M. Simons, *Pure Appl. Chem.* **1999**, *71*, 1249.
- [53] G. J. Tawa, I. A. Topol, S. K. Burt, R. A. Caldwell, A. A. Rashin, *J. Chem. Phys.* **1998**, *109*, 4852.
- [54] (a) C. G. Zhan, D. A. Dixon, *J. Phys. Chem. A* **2001**, *105*, 11534; (b) C. G. Zhan, D. A. J. Dixon, *J. Phys. Chem. B* **2003**, *107*, 4403.
- [55] J. Rimarcik, V. Lukeš, E. Klein, M. Ilcin, *J. Mol. Struct.: Theochem.* **2010**, *925*, 25.
- [56] W. D. Parker, *J. Am. Chem. Soc.* **1992**, *114*, 7458.

- [57] H. Gai, B. C. Garrett, *J. Phys. Chem.* **1994**, 98, 9642.
- [58] A. Galano, R. Álvarez-Diduk, M. T. Ramírez-Silva, G. Alarcón-Ángeles, A. Rojas-Hernández, *Chem. Phys.* **2009**, 363, 13.
- [59] (a) E. Klein, V. Lukeš, *J. Phys. Chem. A* **2006**, 110, 12312, 12320; (b) E. Klein, V. Lukeš, *J. Mol. Struct.: Theochem.* **2006**, 767, 43; (c) E. Klein, V. Lukeš, *Chem. Phys.* **2006**, 330, 515; (d) E. Klein, V. Lukeš, M. Ilcin, *Chem. Phys.* **2007**, 336, 51.
- [60] (a) M. Leopoldini, I. P. Pitarch, N. Russo, M. Toscano, *J. Phys. Chem. A* **2004**, 108, 92; (b) M. Leopoldini, T. Marino, N. Russo, M. Toscano, *J. Phys. Chem. A* **2004**, 108, 4916; (c) M. Leopoldini, T. Marino, N. Russo, M. Toscano, *Theor. Chem. Acc.* **2004**, 111, 210.
- [61] P. Trouillas, P. Marsal, D. Siri, R. Lazzaroni, J. L. Duroux, *Food Chem.* **2006**, 97, 679.
- [62] A. K. Chandra, T. Uchimaru, *Int. J. Mol. Sci.* **2002**, 3, 407.
- [63] (a) M. Najafi, M. Zahedi, E. Klein, *Comput. Theor. Chem.* **2011**, 978, 16; (b) M. Najafi, E. Nazarpour, K. H. Mood, M. Zahedi, E. Klein, *Comput. Theor. Chem.* **2011**, 965, 114; (c) J. Rimarcik, V. Lukeš, E. Klein, L. Rottmannová, *Comput. Theor. Chem.* **2011**, 967, 273.
- [64] Y. Fang, L. Liu, Y. Feng, X.-S. Li, Q.-X. Guo, *J. Phys. Chem. A* **2002**, 106, 4669.
- [65] Z. S. Marković, J. M. D. Marković, C. B. Dolićanin, *Theor. Chem. Acc.* **2010**, 127, 69.
- [66] J. M. Mayer, D. A. Hrovat, J. L. Thomas, W. T. Borden, *J. Am. Chem. Soc.* **2002**, 124, 11142.
- [67] F. Turecek, E. A. Syrstad, *J. Am. Chem. Soc.* **2003**, 125, 3353.
- [68] (a) Y. Feng, L. Liu, Y. Fang, Q.-X. Guo, *J. Phys. Chem. A* **2002**, 106, 11518; (b) Y. Feng, L. Liu, J.-T. Wang, S.-W. Zhao, Q.-X. Guo, *J. Org. Chem.* **2004**, 69, 3129.
- [69] G. S. Hammond, *J. Am. Chem. Soc.* **1955**, 77, 334.

Received: 2 November 2011
Revised: 28 January 2012
Accepted: 31 January 2012
Published online on 16 March 2012